

A: Environmental, Combustion, and Atmospheric Chemistry; Aerosol Processes,
Geochemistry, and Astrochemistry

Rate Coefficient and Mechanism of the OH-Initiated Degradation of 1-Chlorobutane: Atmospheric Implications

Rafael A. Jara-Toro, Javier A. Barrera, Juan P. Aranguren-Abrate, Raúl A. Taccone, and Gustavo A. Pino

J. Phys. Chem. A, **Just Accepted Manuscript** • DOI: 10.1021/acs.jpca.9b10426 • Publication Date (Web): 11 Dec 2019

Downloaded from pubs.acs.org on December 12, 2019

Just Accepted

“Just Accepted” manuscripts have been peer-reviewed and accepted for publication. They are posted online prior to technical editing, formatting for publication and author proofing. The American Chemical Society provides “Just Accepted” as a service to the research community to expedite the dissemination of scientific material as soon as possible after acceptance. “Just Accepted” manuscripts appear in full in PDF format accompanied by an HTML abstract. “Just Accepted” manuscripts have been fully peer reviewed, but should not be considered the official version of record. They are citable by the Digital Object Identifier (DOI®). “Just Accepted” is an optional service offered to authors. Therefore, the “Just Accepted” Web site may not include all articles that will be published in the journal. After a manuscript is technically edited and formatted, it will be removed from the “Just Accepted” Web site and published as an ASAP article. Note that technical editing may introduce minor changes to the manuscript text and/or graphics which could affect content, and all legal disclaimers and ethical guidelines that apply to the journal pertain. ACS cannot be held responsible for errors or consequences arising from the use of information contained in these “Just Accepted” manuscripts.

1
2
3 **Rate Coefficient and Mechanism of the OH-Initiated Degradation of**
4 **1-Chlorobutane: Atmospheric Implications**
5
6
7

8 Rafael A. Jara-Toro,^{a,b,c} Javier A. Barrera,^{a,b,c} Juan P. Aranguren-Abrate,^{a,b,c} Raúl A.
9 Taccone^{a,b,c} and Gustavo A. Pino^{a,b,c,*}
10
11
12

13
14 *a- INFIQC: Instituto de Investigaciones en Fisicoquímica de Córdoba (CONICET –*
15 *UNC) - Haya de la Torre y Medina Allende, Ciudad Universitaria, X5000HUA Córdoba,*
16 *Argentina.*
17

18
19 *b- Departamento de Fisicoquímica, Facultad de Ciencias Químicas – Universidad*
20 *Nacional de Córdoba – Haya de la Torre y Medina Allende, Ciudad Universitaria,*
21 *X5000HUA Córdoba, Argentina.*
22

23
24 *c- Centro Láser de Ciencias Moleculares - Universidad Nacional de Córdoba - Haya*
25 *de la Torre s/n, Pabellón Argentina, Ciudad Universitaria, X5000HUA Córdoba,*
26 *Argentina.*
27

28
29 ** Corresponding Author*

30 *Email: gpino@fcq.unc.edu.ar*
31
32
33
34
35
36
37
38
39
40
41
42
43
44
45
46
47
48
49
50
51
52
53
54
55
56
57
58
59
60

Abstract

In this work, we investigate the degradation process of 1-chlorobutane, initiated by OH radicals, under atmospheric conditions (air pressure of 750 Torr and 296 K) from both experimental and theoretical approaches. In the first one, a relative kinetic method was used to obtain the rate coefficient for this reaction, while the products were identified for the first time (1-chloro-2-butanone, 1-chloro-2-butanol, 4-chloro-2-butanone, 3-hydroxy-butanaldehyde and 3-chloro-2-butanol) using mass spectrometry allowing suggesting a reaction mechanism. The theoretical calculations, for the reactive process, were computed using BHandHLYP/6-311++G(d,p) level of theory and the energies for all the stationary points were refined at the CCSD(T) level. Five conformers for 1-chlorobutane and 33 reactive channels with OH radicals were found, that were considered to calculate the thermal rate coefficient (as the sums of the site-specific rate coefficients, using canonical transition state theory). The theoretical rate coefficient ($1.8 \times 10^{-12} \text{ cm}^3 \text{ molecule}^{-1} \text{ s}^{-1}$) is in good agreement with the experimental value ($2.22 \pm 0.50 \times 10^{-12} \text{ cm}^3 \text{ molecule}^{-1} \text{ s}^{-1}$) determined in this work. Finally, environmental impact indexes were calculated and a discussion on the atmospheric implications due to the emissions of this compound into the troposphere is given.

1. Introduction

Chemical industries produce many halo-alkanes, which are used as organic solvents, degreasing agents, pesticides and intermediates for the synthesis of other organic compounds.^{1,2} As with other industrial chemicals, these compounds have caused numerous cases of environmental pollution due to inadequate waste disposal, accidental discharges or intentional release.^{1,3,4} From this perspective and as a consequence of the degradation processes of halogenated compounds, the accumulation of these species in the troposphere has received considerable attention since they could be transported to the stratosphere contributing to the ozone layer depletion. Therefore, the gas phase kinetic and mechanistic studies of the reactions of halo-alkanes with the most relevant tropospheric oxidants (OH, Cl, NO₃ and O₃) are essential to evaluate their reactivity, the atmospheric destiny and its potential impacts on the quality of the air and the living beings. Especially important is the reaction with the OH radical since it is the main reactive species that initiates the atmospheric degradation of pollutants during the day.

In particular, 1-chlorobutane (C₄H₉Cl or ClBut) is used as an intermediate product for the synthesis of catalysts and other compounds in the chemical industry. It is produced in closed systems, and there are no available data for consumers use. Based on the available information, it is known that its production volume was approximately 800 tons year⁻¹ between 1990-1993 only in Japan,⁵ so that, it should be considered for a systematic study. So far, there are only two previous kinetic studies for the reaction between ClBut and OH radicals to compare with the present measurements.^{6,7} Markert and Nielsen reported a rate coefficient of $k = (1.67 \pm 0.40) \times 10^{-12} \text{ cm}^3 \text{ molecule}^{-1} \text{ s}^{-1}$ at room temperature and atmospheric pressure,⁶ determined by pulsed radiolysis combined with kinetics UV spectroscopy with an excess of water as precursor of the OH radical. A few years later Loison *et al.*,⁷ performed another absolute determination of the rate coefficient for this reaction by means of Pulsed Laser Photolysis coupled to Laser Induced Fluorescence detection of the OH radical (PLP-LIF) and reported a slightly higher value of $k = (2.00 \pm 0.15) \times 10^{-12} \text{ cm}^3 \text{ molecule}^{-1} \text{ s}^{-1}$. The latter value is in very good agreement with the value estimated by the structure-activity relationship (SAR) by the same authors ($k_{\text{SAR}} = 1.97 \times 10^{-12} \text{ cm}^3 \text{ molecule}^{-1} \text{ s}^{-1}$).⁷

Considering the fact that none of the reported values were determined under atmospheric conditions and that the degradation products remain unknown, we proceeded to re-determine the rate coefficient for the title reaction using a relative method, under atmospheric pressure in air and to identify the products of the reaction that will allow suggesting a likely reaction mechanism. The experimental results were complemented with electronic structure

calculations to explore the relevant points on the potential energy surface (PES) of the reaction and the reaction rate coefficient was calculated with the transition state theory (TST).

Finally, the atmospheric lifetime (τ), Radiative Efficiency (RE), Global Warming Potential (GWP), Ozone Depletion Potential (ODP) and Photochemical Ozone Creation Potential index (POCP_E) were evaluated using the experimental results from this work, contributing to a better understanding of the atmospheric chemistry of halo-alkanes.

2. Methodology

Kinetic measurements

The rate coefficient for the title reaction at (296 ± 2) K and atmospheric pressure (750 ± 10) Torr was determined by the conventional relative rate method described in previous works.⁸⁻¹²

The decay of the concentration of ClBut from reaction R.2.1 is determined relative to the decay of the concentration of a reference compound (Ref) ($n\text{-C}_5\text{H}_{12}$ and $\text{iso-C}_3\text{H}_7\text{OH}$) from R.2.2.



If the decay of ClBut and Ref is only given by reactions R.2.1 and R.2.2 with the OH radical, the following relationship can be established:

$$\text{Ln} \left(\frac{[\text{ClBut}]_0}{[\text{ClBut}]_t} \right) = \frac{k_{\text{ClBut}}}{k_{\text{Ref}}} \text{Ln} \left(\frac{[\text{Ref}]_0}{[\text{Ref}]_t} \right) \quad (\text{Eq. 1})$$

where $[\text{ClBut}]_0$, $[\text{ClBut}]_t$, $[\text{Ref}]_0$ and $[\text{Ref}]_t$ are the ClBut and Ref concentrations at time zero (t_0) and at any time (t), respectively. From Eq. 1, k_{ClBut} is obtained from the slope $\frac{k_{\text{ClBut}}}{k_{\text{Ref}}}$ of a plot of $\text{Ln} \left(\frac{[\text{ClBut}]_0}{[\text{ClBut}]_t} \right)$ vs. $\text{Ln} \left(\frac{[\text{Ref}]_0}{[\text{Ref}]_t} \right)$, owing that the values of k_{ref} are known ($k_{n\text{-C}_5\text{H}_{12}} = (3.96 \pm 0.79) \times 10^{-12} \text{ cm}^3 \text{ molecule}^{-1} \text{ s}^{-1}$)¹³ and $k_{\text{iso-C}_3\text{H}_7\text{OH}} = (5.1 \pm 1.3) \times 10^{-12} \text{ cm}^3 \text{ molecule}^{-1} \text{ s}^{-1}$)¹⁴).

The experimental setup was described in detail previously and only a brief description will be given here.⁸⁻¹² The kinetic determinations were made in a collapsible Teflon bag of approximately 80 L. All the reactants diluted in ultra-pure air were left to mix in the reaction chamber for approximately 1 h before the first photolysis. The OH radicals were produced by

1
2
3 the UV photolysis of H₂O₂ at around 254 nm for which the Teflon bag was placed inside a
4
5 wooden box with six germicidal lamps (Philips 30 W). The interior walls of the photolysis box
6
7 were covered with aluminum foils.
8

9 Mixtures of ClBut, Ref and H₂O₂ were irradiated for 5 or 6 periods of 2 min, up to 10 or
10
11 12 min of total photolysis. After each irradiation period, the concentrations of ClBut and Ref
12
13 were determined by gas chromatography (GC) with a gas chromatograph with flame ionization
14
15 detection (GC-FID) Perkin Elmer Clarus 500. This GC-FID had an Elite 5 capillary column (30 m
16
17 x 0.32 mm DI x 0.25 μm) that supports a maximum temperature of 350 °C. Samples were taken
18
19 from the reactor and incorporated into the chromatograph using a gas-tight syringe Hamilton
20
21 with a volume of 5 mL.

22 After each experiment, the bag was cleaned by a continuous flow of ultra-pure air until
23
24 the appropriate humidity conditions (< 5% RH) were achieved and the absence of ClBut and the
25
26 others compounds that may have been adsorbed on its walls was corroborated.

27 **Analysis of reaction products**

28 The reaction products were identified by gas chromatography coupled to quadrupole
29
30 mass spectrometry (GC-MS), using a gas chromatograph Clarus 500 Perkin Elmer coupled to a
31
32 mass spectrometer Clarus 560 S Perkin Elmer (GC-MS). The analysis of the results was carried
33
34 out by the software TurboMass™ GC/MS version 5.4.2, provided by the manufacturer.
35

36 **Chemicals**

37 The chemicals used were N₂ (Linde 99.999%. CAS: 7727-37-9), ultra-pure air (synthetic
38
39 air), C₄H₉Cl (Sigma aldrich 99.5%. CAS: 109-69-3), H₂O₂ (70.5%. CAS: 7722-84-1) supplied by
40
41 Atanor S.A. The solution of H₂O₂ was bubbled with high purity N₂ during 3-4 days before using it
42
43 in order to reduce the H₂O content. Since H₂O₂ cannot be obtained free of H₂O, its
44
45 concentration was determined by standard titration with KMnO₄ and typically, the content of H₂O
46
47 was less than 10% wt. n-C₅H₁₂ (98%. CAS: 109-6-0) and iso-C₃H₇OH (>98%. CAS: 67-63-0)
48
49 were supplied by Sigma Aldrich. The reactants were degassed by repeated freeze-pump-thaw
50
51 cycling and purified by vacuum distillation until GC revealed no observable impurities.

52 **Computational**

53 The OH + ClBut reaction has been studied at the density functional theory (DFT) level,
54
55 using the BHandHLYP functional with the 6-311++G(d,p) basis set in Gaussian09 program.¹⁵
56
57

1
2
3 Conformational analysis for ClBut and the molecular properties (geometries, vibrational
4 frequencies and thermodynamic values) for all stationary points in the possible reaction
5 channels have been calculated and the electronic energies (EE) were corrected at CCSD(T)
6 level.
7
8

9 The CCSD(T)/6-311++G(d,p)//BHandHLYP/6-311++G(d,p) method has been chosen
10 since Alvarez-Idaboy *et al.* have previously shown that it renders satisfactory results for the
11 modeling of oxidation reactions of volatile organic compounds (VOCs).^{16,17}
12
13

14 The identity of stationary points was determined by a frequency analysis (zero or one
15 imaginary frequency for a minimum or transition state, respectively). The theoretical rate
16 coefficient for all reaction channels was calculated using the conventional transition state theory
17 with Wigner tunnel transmission coefficient.^{18–20}
18
19
20
21

22 3. Results

23 Rate coefficient determination

24 The rate coefficient for R.2.1 (OH + ClBut) at 296 ± 2 K was determined by the relative
25 method described in the previous section. Several experiments were performed prior to the
26 kinetic determinations in order to ensure that the depletion rate of ClBut and the Ref compounds
27 by photolysis, wall reactions and dark reactions are negligible as compared with the reaction
28 with the OH radicals. Two different reference compounds were used to determine the value of
29 the rate coefficient of the reaction: n-C₅H₁₂ and iso-C₃H₇OH whose rate coefficients for the
30 oxidation by OH radicals under dry conditions are: $k_{n-C_5H_{12}} = (3.96 \pm 0.79) \times 10^{-12} \text{ cm}^3 \text{ molecule}^{-1}$
31 s^{-1} ¹³ and $k_{iso-C_3H_7OH} = (5.1 \pm 1.3) \times 10^{-12} \text{ cm}^3 \text{ molecule}^{-1} \text{ s}^{-1}$ ¹⁴, respectively.
32
33
34
35
36
37

38 The initial concentrations of ClBut, n-C₅H₁₂ and iso-C₃H₇OH were 9.8×10^{14} molecules
39 cm^{-3} , whereas the concentration of H₂O₂ was 3.2×10^{17} molecules cm^{-3} .
40

41 Figure 1 shows a typical graph of $\text{Ln} \left(\frac{[\text{ClBut}]_0}{[\text{ClBut}]_t} \right)$ vs. $\text{Ln} \left(\frac{[\text{Ref}]_0}{[\text{Ref}]_t} \right)$ (Eq. 1), for determinations
42 using both Ref compounds.
43
44
45
46
47
48
49
50
51
52
53
54
55
56
57
58
59
60

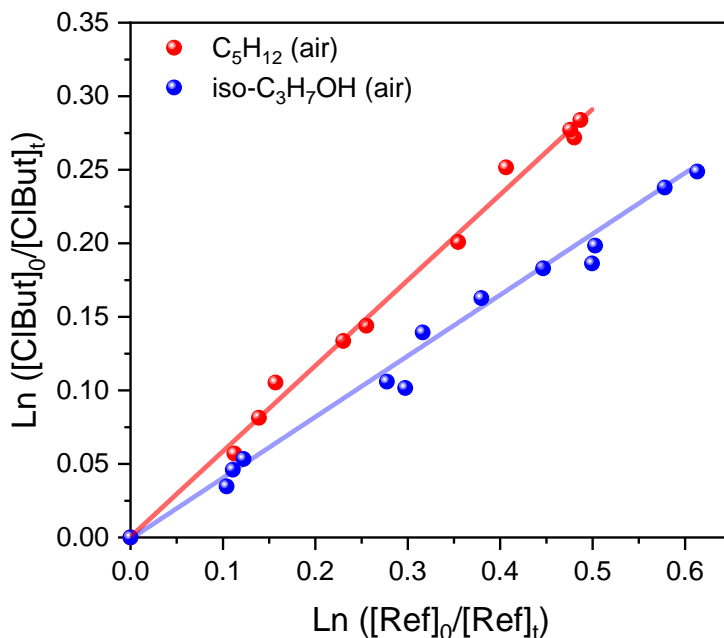


Figure 1. Typical relative kinetic plot for the ClBut + OH reaction at 296 ± 2 K and atmospheric pressure, with two different reference compounds as indicated in the plot.

The rate coefficient for the reaction ClBut + OH determined against different Ref compounds are reported in Table 1. The average value of this rate coefficient taking into account the multiple determinations with both Ref was $(2.22 \pm 0.50) \times 10^{-12} \text{ cm}^3 \text{ molecule}^{-1} \text{ s}^{-1}$, in agreement with one of the previously reported value $(2.00 \pm 0.15) \times 10^{-12} \text{ cm}^3 \text{ molecule}^{-1} \text{ s}^{-1}$.⁷ The reported errors were determined by the propagation of the uncertainties of independent variables according to the following equation:

$$\Delta k = \sqrt{\left[\left(\frac{\Delta S}{S}\right)^2 + \left(\frac{\Delta k_{\text{Ref}}}{k_{\text{Ref}}}\right)^2\right]} * k \quad (\text{Eq. 2})$$

where, ΔS is $2\sigma_{n-1}$ of the slope (S) of the plots shown in Figures 1, obtained from the least squares fit, and k_{Ref} and Δk_{Ref} refers to the rate coefficient of the reference reaction and its associated uncertainty, respectively and k is the rate coefficient determined in each experiment.

Table 1. Rate coefficients, k_{ClBut} , for the ClBut + OH reaction at 296 K and atmospheric pressure.

Ref.	k_{Ref} ($\times 10^{-12} \text{ cm}^3 \text{ molecule}^{-1} \text{ s}^{-1}$)	k_{ClBut} ($\times 10^{-12} \text{ cm}^3 \text{ molecule}^{-1} \text{ s}^{-1}$)
C ₅ H ₁₂	3.96 ± 0.79	2.35 ± 0.50
iso-C ₃ H ₇ OH	5.1 ± 1.3	2.1 ± 0.5

$$\text{Average } k_{\text{ClBut}} = (2.22 \pm 0.50) \times 10^{-12} \text{ cm}^3 \text{ molecule}^{-1} \text{ s}^{-1}$$

Reaction Products

To obtain some information about the reaction mechanism and the OH-initiated degradation pathways of ClBut in presence of O₂, the reaction products were identified by GC-MS under the same experimental conditions of the kinetic determinations in pure air and after 8 min of irradiation in the absence of the reference compound.

A typical FID chromatogram is presented in Figure 2, together with the assignment of each peak. The total ions chromatogram (TIC) and the corresponding mass spectra are shown in the Supporting Information (Figures S1 to S7). The assignment of each mass spectrum was achieved by comparison of those stored in the NIST database (NIST mass spectral search program, ver. 2.0d),²¹ which allowed identifying the following reaction products: 1) 1-chloro-2-butanone, 2) 1-chloro-2-butanol, 3) 4-chloro-2-butanone, 4) 3-hydroxy-butanaldehyde and 5) 3-chloro-2-butanol.

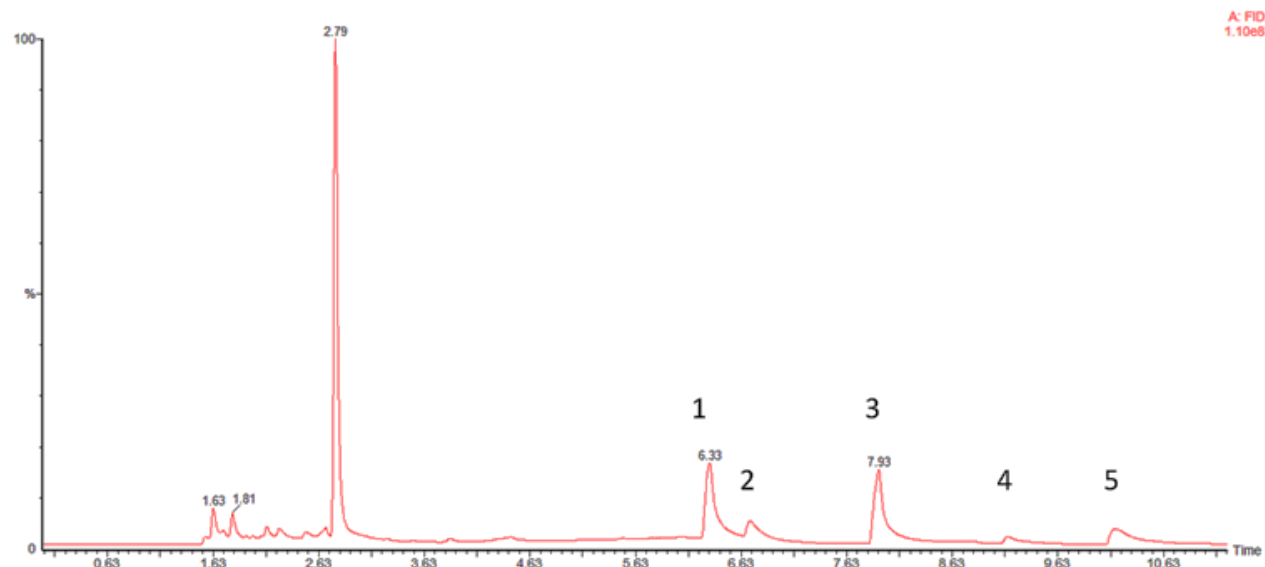


Figure 2. The typical chromatogram obtained by FID detection for ClBut + OH reaction. The reaction was performed in the absence of Ref compound, in air bath gas and 8 min of irradiation.

Although the quantification of the products was not carried out, a qualitative analysis of the relative intensities of the chromatographic peaks (FID and TIC) shows that those corresponding to 1) 1-chloro-2-butanone and 3) 4-chloro-2-butanone are the most intense one. Considering similar sensitivities for all these compounds, it can be assumed that these two products are at a higher concentration than the others and then, they are the main products of the reaction.

Theoretical

To shed some light into the reaction mechanism and final products distribution, electronic structure calculations were performed on the conformation of the reactant molecule and possible reaction pathways with the OH radical, exploring the stationary points of the PES of the reactions.

Given the flexibility of ClBut and the existence of different conformers according to previous reports,^{22–26} a conformational analysis of this molecule was carried out in order to obtain information regarding the populations of the different conformers at the temperature of the present work. In this sense, the dihedral angles for the C_{α} - C_{β} and C_{β} - C_{γ} bonds were scanned from -180° to 180° and 5 stable conformers were found as shown in Figure 3. The

labels used for each conformer refers to the orientation anti (*a*) or gauche (*g*) of the Cl-atom and the terminal CH₃ group, indicated in this order.

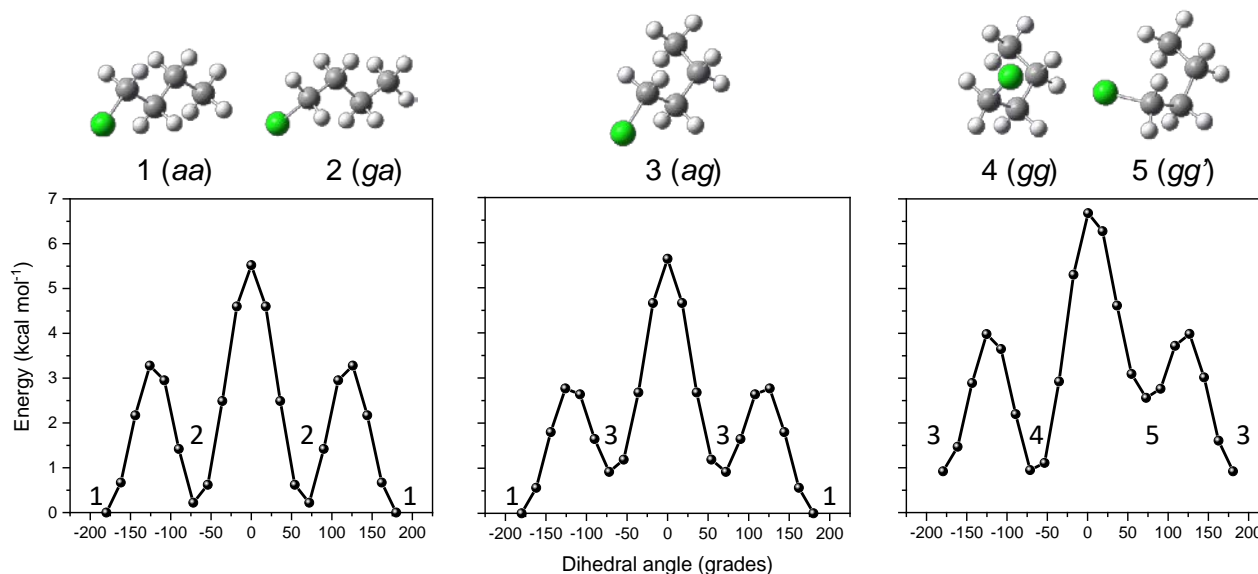
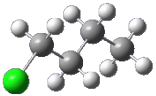
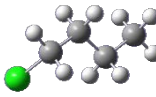
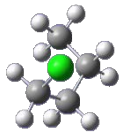
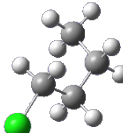
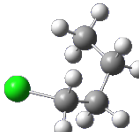


Figure 3. Relative electronic energy profile + ZPE for the conformational isomerization of ClBut as a function of the C_α-C_β and C_β-C_γ dihedral angles obtained at the BHandHLYP/6-311++G(d,p) level.

The standard Gibbs free energy at 296 K (G°_{296K}) for all the conformers was calculated at the BHandHLYP/6-311++G(d,p) level and refined at the CCSD(T)/6-311++G(d,p) level, using the rigid rotor and harmonic oscillator approximations for the calculation of the partition functions. The G°_{296K} values relative to the most stable *aa* conformer (ΔG°_{296K}) are shown in Table 2 as well as their relative population at the same temperature, considering a Boltzmann distribution.

As observed in Table 2, the *aa* conformer is the most stable one, irrespective of the level of theory used, but none of them have significant differences with respect to others. The relative populations do not depend very much on the level of theory, for this reason, the calculations on the reactivity were carried out considering the population of all conformers determined at the CCSD(T)/6-311++G(d,p) level.

Table 2. ΔG°_{296K} and relative abundance, of the different conformations, of ClBut calculated by BHandHLYP/6-311++G(d,p) and CCSD(T)/6-311++G(d,p)//BHandHLYP/6-311++G(d,p) level of theory.

Conformer	BHandHLYP		CCSD(T)//BHandHLYP	
	ΔG°_{296K} (kcal mol ⁻¹)	Relative Population	ΔG°_{296K} (kcal mol ⁻¹)	Relative Population
 (aa)	0.0	45.6	0.0	35.2
 (ga)	0.2	32.4	0.1	31.5
 (gg)	0.9	10.6	0.3	20.7
 (ag)	0.9	10.7	0.7	11.4
 (gg')	2.5	0.7	2.0	1.2

1
2
3 The primary and rate limiting step for reactions of alkanes with the OH radical is the H-
4 atom abstraction to produce H₂O and an alkyl radical R that in air proceeds to products through
5 reaction with O₂. In the case of ClBut, the H abstraction can take place at different positions: C_α,
6 C_β, C_γ and C_δ.
7

8
9 A comprehensive search of the different reaction channels was performed at the
10 BHandHLYP/6-311++G(d,p) level for the 5 conformers. This search led to 33 total reaction
11 channels and all of them start with the formation of a pre-reactive complex (CR) stabilized by a
12 H-bond interaction between the Cl-atom and the OH radical which lies within a range of 2.44 -
13 0.80 kcal/mol below the reactants energy. The energy of the stationary points on the PES
14 (reactants, CR, transition state (TS) and product complex (CP)) was refined at the
15 CCSD(T)//BHandHLYP level for the 33 channels and the results for the conformers at both
16 theory level are shown in Figure 4.
17
18

19 The sub-indexes *i* and *j* in the label of the stationary points CR_{*ij*}, TS_{*ij*} and CP_{*ij*} indicate the
20 conformation of ClBut, *i* = *aa*, *ga*, *ag*, *gg* or *gg'* and the abstraction position *j* = α_{*n*}, β_{*n*}, γ_{*n*} and δ_{*n*}.
21 The number *n* = 1, 2 stands for the H abstraction in the same plane of the Cl-atom or in the
22 opposite one, respectively; while *n* = 3 stands for the abstraction of the remaining H in the
23 terminal C_δH₃ group only.
24
25

26 The structures of the CR_{*ij*}, TS_{*ij*} and CP_{*ij*} and their corresponding relative energies are
27 shown in Tables S1 and S2. The abstractions of H from C_β and C_γ are the most favorable. As
28 will be discussed in Section 4, these abstraction channels allow the formation of the main
29 reaction products, 4-chloro-2-butanone and 1-chloro-2-butanone as well as 1-chloro-2-butanol.
30
31

32 However, the formation of 3-hydroxy-butanaldehyde and 3-chloro-2-butanol requires the
33 elimination of the Cl-atom or its migration from C_α to C_β and it will be discussed with the reaction
34 mechanism.
35
36
37
38
39
40
41
42
43
44
45
46
47
48
49
50
51
52
53
54
55
56
57
58
59
60

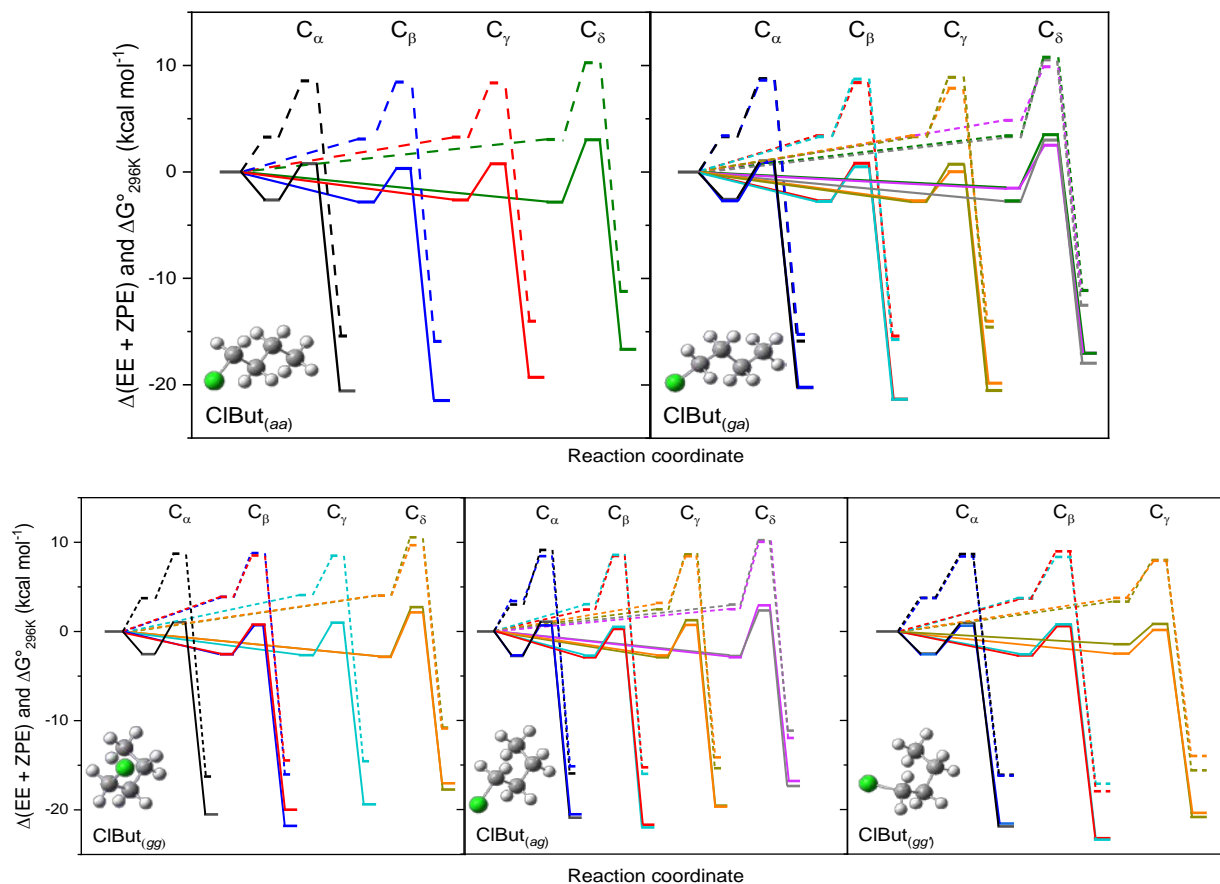


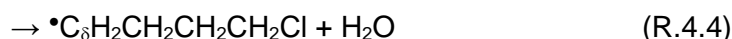
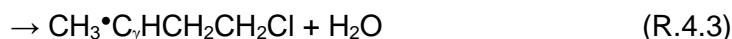
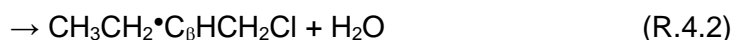
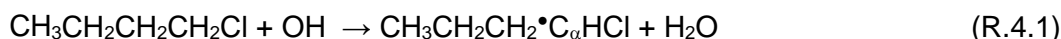
Figure 4. Relative electronic energies including ZPE correction (full lines) and ΔG°_{296K} (dashed lines) (in kcal mol⁻¹) for the stationary points calculated at the CCSD(T)//BHandHLYP level of theory for the reaction CIBut + OH, for the five conformers of CIBut as indicated.

4. Discussion

The rate coefficient determined at 296 K for the reaction CIBut + OH $k = (2.22 \pm 0.50) \times 10^{-12} \text{ cm}^3 \text{ molecule}^{-1} \text{ s}^{-1}$ is in very good agreement with one of the previously determined values $(2.00 \pm 0.15) \times 10^{-12} \text{ cm}^3 \text{ molecule}^{-1} \text{ s}^{-1}$.⁷ It should be noted that the agreement with the another previously reported value⁶ $(1.67 \pm 0.4) \times 10^{-12} \text{ cm}^3 \text{ molecule}^{-1} \text{ s}^{-1}$ is still within the experimental error. This latter value was determined under very high concentrations of H₂O since this compound was used as a radiolytic precursor of the OH radical. Given the catalytic^{8,9,27} and anticatalytic^{27,28} effect of H₂O on organic compounds reactions, this could be a reason of the observed difference.

Rate coefficient calculation

As mentioned in section 3, the first H-atom abstraction by the OH radical from the ClBut is the rate limiting step as also shown by electronic structure calculations (Figures 4) leading to the formation of the corresponding alkyl radical according to the following reactions:



The rate coefficient for the title reaction was calculated by the conventional Transition State Theory (TST), considering the energetic of all the reaction channels of the five conformers of ClBut at 296 K.

The rate coefficients k_{ij} for each j reaction channel (abstraction position) of the i conformers were calculated according to the following equation (Eq. 3):

$$k_{ij} = \Gamma_{ij} \frac{k_B T}{h} e^{\left(-\frac{\Delta G_{ij}^{\ddagger}}{N_A k_B T} \right)} \quad (\text{Eq. 3})$$

where Γ is the tunnel transmission coefficient calculated by the Wigner method,²⁰ k_B , h and N_A are the Boltzmann's, Plank's and Avogadro's constants, respectively; T is the temperature of the system and ΔG_{ij}^{\ddagger} stands for the standard Gibbs free energy of activation calculated at the CCSD(T)/6-311++G(d,p)//BHandHLYP/6-311++G(d,p) level of theory and reported in Table 3 together with the calculated k_{ij} .

Thus, the total rate coefficient (k_{total}) for the reaction at 296 K was calculated as the sum of the k_{ij} coefficients for each reaction channel weighted by the relative population of the corresponding conformer P_i , according to Eq. 4:

$$k_{\text{total}} = \sum_i (\sum_j k_{ij}) P_i \quad (\text{Eq. 4})$$

A close inspection to Table 3 shows, as a general trend, that the hydrogen abstraction to C_γ (R.4.3) renders the highest rate coefficients, while those for the abstraction on C_α and C_β are slightly smaller. The theoretical branching ratios ($Y = k_{\text{C}_n}/k_{\text{total}}$) for abstraction on each C_n are:

1
2
3 $Y_{C\gamma} = 0.37 > Y_{C\beta} = 0.31 \geq Y_{C\alpha} = 0.30 \gg Y_{C\delta} = 0.02$, indicating that the only negligible channel is
4 the abstraction on C_{δ} .
5

6 Calculations show that H abstraction from C_{β} and C_{γ} is energetically favored comprising
7 the lowest energy barriers due to the inductive effect (-I) of the Cl-atom. The electron density is
8 highly localized on the electronegative Cl-atom, which strengthens the C-H bonds, where this
9 effect is stronger in those C-H bonds which are closer to Cl, being consistent with the
10 hypothesis proposed by Market and Nielsen.⁶ Therefore, the reactivity toward the OH radical
11 increases $C_{\alpha} < C_{\beta} < C_{\gamma}$. The exception is the abstraction from the terminal $C_{\delta}H_3$ group since the
12 TS is very similar to the unstable primary alkyl radical produced as intermediate and then it is
13 the least reactive position.
14
15

16 From Table 3 it is also observed that the gg' conformer renders the largest global rate
17 coefficient ($k_i = \sum_j k_{ij} = 3.1 \times 10^{-12} \text{ cm}^3 \text{ molecule}^{-1} \text{ s}^{-1}$) among all conformers. However, its
18 population is very low as compare to the population of the other 4 conformers and then, its
19 contribution to the total rate coefficient is negligible. The main contribution to the total rate
20 coefficient comes from the aa and ga conformers, which in turn are the most populated ones.
21
22

23 The total rate coefficient calculated according to Eq. 4 ($k_{total} = 1.8 \times 10^{-12} \text{ cm}^3 \text{ molecule}^{-1}$
24 s^{-1}) is in very good agreement with the experimental value ($(2.22 \pm 0.50) \times 10^{-12} \text{ cm}^3 \text{ molecule}^{-1}$
25 s^{-1}).
26
27
28
29
30
31
32
33
34
35
36
37
38
39
40
41
42
43
44
45
46
47
48
49
50
51
52
53
54
55
56
57
58
59
60

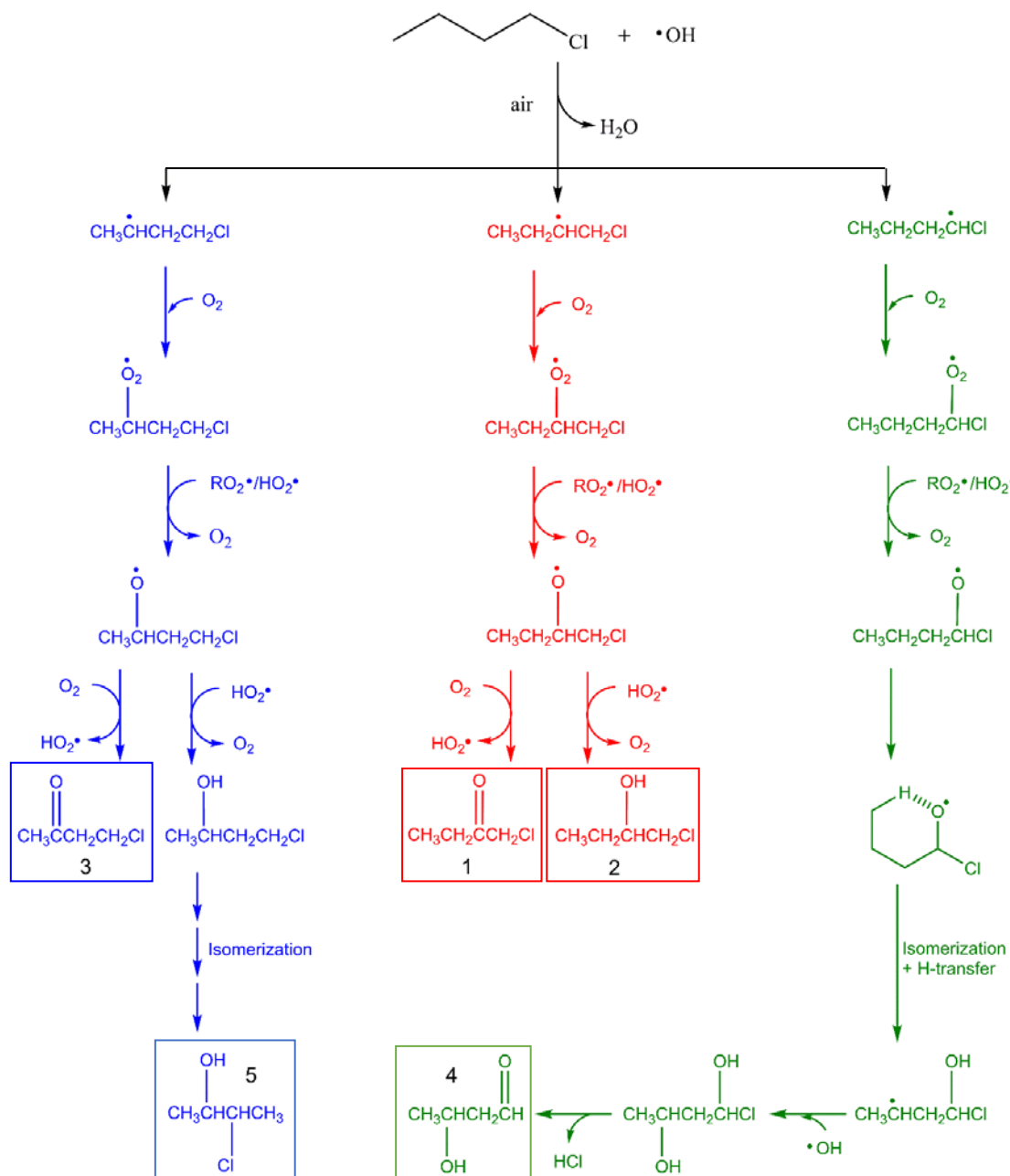
Table 3. ClBut conformer's populations (P) and standard Gibbs free energy of activation (ΔG^\ddagger), tunneling corrections (Γ) and rate coefficients (k_{ij}) at 296 K for the reaction ClBut + OH at CCSD(T)/6-311++G(d,p)//BHandHLYP/6-311++G(d,p) level of theory.

Atom	Conformer <i>aa</i> $P_{aa} = 0.35$			Conformer <i>ga</i> $P_{ga} = 0.32$			Conformer <i>ag</i> $P_{ag} = 0.11$			Conformer <i>gg</i> $P_{gg} = 0.21$			Conformer <i>gg'</i> $P_{gg'} = 0.01$			$k(C_n)^a$
	ΔG^\ddagger (kcal mol ⁻¹)	Γ_{ij}	k_{ij}^a	ΔG^\ddagger (kcal mol ⁻¹)	Γ_{ij}	k_{ij}^a	ΔG^\ddagger (kcal mol ⁻¹)	Γ_{ij}	k_{ij}^a	ΔG^\ddagger (kcal mol ⁻¹)	Γ_{ij}	k_{ij}^a	ΔG^\ddagger (kcal mol ⁻¹)	Γ_{ij}	k_{ij}^a	$n=\alpha, \beta, \gamma, \delta$
Cα-1	8.5	3.7	1.2x10 ⁻¹³	8.8	3.8	8.2x10 ⁻¹⁴	9.1	4.0	4.3x10 ⁻¹⁴	8.7	3.8	9.1x10 ⁻¹⁴	8.7	3.2	9.5x10 ⁻¹⁴	5.5x10⁻¹³
Cα-2	-----	-----	-----	8.6	3.8	1.1x10 ⁻¹³	8.4	3.7	1.4x10 ⁻¹³	-----	-----	-----	8.4	3.6	1.5x10 ⁻¹³	
Cβ-1	8.4	3.6	1.5x10 ⁻¹³	8.4	2.9	7.3x10 ⁻¹⁵	8.5	3.6	1.4x10 ⁻¹³	8.8	3.7	8.1x10 ⁻¹⁴	9.0	3.9	5.7x10 ⁻¹⁴	5.6x10⁻¹³
Cβ-2	-----	-----	-----	8.7	3.7	9.1x10 ⁻¹⁴	8.6	3.6	1.1x10 ⁻¹³	8.5	2.9	1.3x10 ⁻¹³	8.3	2.8	1.7x10 ⁻¹³	
Cγ-1	8.4	2.7	1.7x10 ⁻¹³	8.9	3.5	6.8x10 ⁻¹⁴	8.6	2.9	1.0x10 ⁻¹³	8.5	2.8	1.3x10 ⁻¹⁴	8.0	2.4	3.0x10 ⁻¹³	6.7x10⁻¹³
Cγ-2	-----	-----	-----	7.9	2.7	3.8x10 ⁻¹³	8.4	2.8	1.5x10 ⁻¹³	-----	-----	-----	7.9	2.6	3.4x10 ⁻¹³	
Cδ-1	10.3	3.6	6.5x10 ⁻¹⁵	10.5	3.6	4.1x10 ⁻¹⁵	10.2	3.5	6.7x10 ⁻¹⁵	10.5	3.5	4.0x10 ⁻¹⁵	-----	-----	-----	4.0x10⁻¹⁴
Cδ-2	-----	-----	-----	9.9	3.4	1.2x10 ⁻¹⁴	10.1	3.6	9.3x10 ⁻¹⁵	-----	-----	-----	-----	-----	-----	
Cδ-3	-----	-----	-----	10.8	3.7	2.7x10 ⁻¹⁵	-----	-----	-----	9.7	3.3	1.8x10 ⁻¹⁴	-----	-----	-----	
	$k_i = \sum k_{ij} \Gamma_{ij}$		1.4x10⁻¹²	$k_i = \sum k_{ij} \Gamma_{ij}$		2.4x10⁻¹²	$k_i = \sum k_{ij} \Gamma_{ij}$		2.4x10⁻¹²	$k_i = \sum k_{ij} \Gamma_{ij}$		1.1x10⁻¹²	$k_i = \sum k_{ij} \Gamma_{ij}$		3.1x10⁻¹²	k_{global}^a
	$k_i \cdot P_i$		5.0x10⁻¹³	$k_i \cdot P_i$		7.7x10⁻¹³	$k_i \cdot P_i$		2.6x10⁻¹³	$k_i \cdot P_i$		2.4x10⁻¹³	$k_i \cdot P_i$		3.1x10⁻¹⁴	1.8 x 10⁻¹²

a) Units in cm³ molecule⁻¹ s⁻¹

Reaction Mechanism

Under the present experimental conditions, the alkyl radicals produced in the first abstraction step will add molecular O_2 to form peroxy radicals. In NO_x -free conditions, the peroxy radicals will react further via peroxy self-reactions producing a large extent of alkoxy radicals. The alkoxy radicals formed can decompose, isomerize or react with O_2 or HO_2 . Considering the theoretical branching ratios reported in the previous section and the identified products, the following reaction mechanism is suggested:



Scheme 1. General mechanism for the formation of observed products in ClBut + OH reaction. Color code indicates the H-abstraction for different C-atoms and the observed products, by GC-MS, are framed and numbered.

The commonly accepted mechanism²⁹ explains the formation of the main products, 1-chloro-2-butanone and 4-chloro-2-butanone as shown in Scheme 1 (products 1 and 3, respectively) by the reaction of the C_γ and C_β alkoxy radicals with O₂. The formation of 1-chloro-2-butanol (product 2) and 3-chloro-2-butanol (product 5) is probably related to competitive reaction of the C_γ and C_β alkoxy radicals with the HO₂ radical, respectively. The latter reaction is likely due to the considerably high steady concentration of the HO₂ radical (in the order of 10¹² radicals cm⁻³) produced as a consequence of the OH + H₂O₂ reaction ($k = (2.00 \pm 0.15) \times 10^{-12} \text{ cm}^3 \text{ molecule}^{-1} \text{ s}^{-1}$),³⁰ and due to the high initial concentration of H₂O₂.

The corresponding alcohol produced by the reaction of the C_γ alkoxy radical with HO₂ was not detected under the present experimental conditions. However, product 5 shows an alcohol group in C_γ followed by a Cl atom migration from C_α to C_β, and then it could be the isomer of the missing product.

A detailed study, by computational calculations, for the reaction of the alkoxy radicals with the HO₂ radical is out of the scope of this work. However, Zhang *et al.*, reported a theoretical study on the HO₂ + C₂H₅O → C₂H₅OH + O₂ reaction finding that the transition state lies at 6.94 kcal/mol below the energy of the reactants, which makes this process very likely.³¹

Additionally, as determined from calculations, abstraction from C_α is not negligible. Thus, we expect that 3-hydroxy-butanaldehyde (product 4) accounts for this reaction channel, whose formation proceed through a six-member-ring intermediate that allows the H-transfer from C_δ to O to produces a primary radical. This primary radical is unstable which drives the H-migration to form the secondary radical, that can undergo subsequent reactions upto the final product 4, as depicted in the proposed mechanism (Scheme 1).

Atmospheric Implications

The atmospheric sink of a VOC is given by several removal processes: photolysis, wet and dry deposition and reactions with the main oxidants of the atmosphere (OH, Cl, NO₃ and O₃).²⁹ Then, the global tropospheric lifetime of ClBut is estimated as the reciprocal of the sum of loss rates of each removal process, according to the following equation:

$$\tau_{global} = \left[\frac{1}{\tau_{OH}} + \frac{1}{\tau_{Cl}} + \frac{1}{\tau_{NO_3}} + \frac{1}{\tau_{O_3}} + \frac{1}{\tau_{photolysis}} + \frac{1}{\tau_{other\ processes}} \right]^{-1} \quad (\text{Eq. 5})$$

Since the photodissociation quantum yield of aliphatic hydrocarbons is extremely small in the actinic region of the lower troposphere and their solubility in water is also low, the photolysis and wet deposition of ClBut are neglected.^{32,33} Unfortunately, the rate

coefficients for the reactions of ClBut with NO₃ and O₃ are unknown. However, a comparison with the corresponding rate coefficients for the reactions with n-butane suggests that the oxidation rate of ClBut by NO₃ and O₃ is very slow to be competitive with the corresponding reactions with Cl and OH.^{34,35} Thus, they can also be neglected in the calculation of τ_{global} . As a consequence, an upper limit for τ_{global} is estimated considering only the oxidation reaction with the most important tropospheric oxidants (Cl and OH). The value of $k_{\text{Cl}} = (1.11 \pm 0.05) \times 10^{-10} \text{ cm}^3 \text{ molecule}^{-1} \text{ s}^{-1}$, reported by other authors³⁶ and the value of $k_{\text{OH}} = (2.22 \pm 0.50) \times 10^{-12} \text{ cm}^3 \text{ molecule}^{-1} \text{ s}^{-1}$ determined in this work were used for the calculation of τ_{global} together with the following recommended global concentrations of the oxidants: a 12 h average day-time concentration for [OH] = $1 \times 10^6 \text{ radical cm}^{-3}$,³⁷ an average global concentration for [Cl]_{avg} = $1.0 \times 10^3 \text{ atom cm}^{-3}$ ³⁸ and a peak concentration [Cl]_{coastal} = $1.3 \times 10^5 \text{ atom cm}^{-3}$ ³⁹ in the coastal marine boundary layer. In this sense, the calculated lifetimes of ClBut were, $\tau_{\text{OH}} = 5.42 \text{ days}$, $\tau_{\text{Cl}_{\text{avg}}} = 105 \text{ days}$ and $\tau_{\text{Cl}_{\text{coastal}}} = 19 \text{ h}$ and a $\tau_{\text{global}}^{\text{avg}} = 4.9 \text{ days}$ and $\tau_{\text{global}}^{\text{coastal}} = 16 \text{ h}$, indicating that the most important tropospheric sink of ClBut is the reaction with the OH radical, except in the coastal marine boundary layer where this compound is essentially oxidized by Cl, due to high concentration of this atom in sea regions.

The very short lifetime of ClBut in the troposphere indicates that only local effects due to its emission are expected.

Photochemical ozone creation potentials index (POCP) is yet another issue that requires consideration in the evaluation of the environmental impact of ClBut.⁴⁰ The POCP for a particular VOC is determined by quantifying the effect of a small incremental in its emission on the calculated amount of ozone formed, relative to that resulting from an identical increase in the emission (on a mass basis) of a reference compound, which is taken to be ethene (POCP = 100).⁴¹ Recently, Jenkin *et al.*⁴⁰ have developed a simple method to estimate the POCP (POCP_E) values of a VOC, rationalized in terms of its chemical structure and reactivity with the OH radical, focused on multiday north-west Europe and single-day USA-urban conditions, according to Eq.6:

$$\text{POCP}_E = A \cdot \gamma_s \cdot R \cdot S \cdot F \quad (\text{Eq. 6})$$

where F takes, by default, a value of 1 except for only a specific series of compounds and A is a multiplier. Parameters R and γ_s are related to structure and reactivity with OH radicals, respectively; while S is related to the size of VOC. These parameters are defined according to Eqs. 7-10, respectively:

$$y_s = (n_B/6) * (28.05/M) \quad (\text{Eq. 7})$$

$$R = 1 - (B * y_R + 1)^{-1} \quad (\text{Eq. 8})$$

$$S = (1 - \alpha) * (-C * n_C^\beta) + \alpha \quad (\text{Eq. 9})$$

$$y_R = (k_{OH} / k_{OH^e}) * (6/n_B) \quad (\text{Eq. 10})$$

M stands for the molar weight, n_C the number of C atoms and n_B is the number of C-C and C-H bonds of the VOC. k_{OH} and k_{OH^e} are the rate coefficients for the reaction of the VOC and the reference compound (ethene, $8.64 \times 10^{-12} \text{ cm}^3 \text{ molecule}^{-1} \text{ s}^{-1}$)¹³ with OH radical at a given temperature.⁴² The B value describes the POCP_E dependency on the OH radical under different atmospheric conditions. Parameters α , β and C are used to describe the dependency of POCP_E on the size of the VOC. The A, B, α , β and C parameters were obtained from Jenkin *et al.*⁴³ and are showed in Table S3.

Thus, the POCP_E for ClBut was estimated as explained above, focused on different timescales (eg: single-day USA urban conditions and multi-days north-west European conditions). In this regard, the POCP_E values obtained for the degradation process of ClBut by OH radicals were 9.29 in single-day USA urban conditions and 18.83 in multi-days north-west European conditions, which are smaller than the corresponding values reported for n-butane (17.1 and 32 under the same conditions, respectively).⁴³ This is in agreement with the study of Cheng *et al.*⁴⁴ in which the authors reported that production of photochemical O₃ from halo-alkanes is less important than from the corresponding alkanes due to the presence of the halogen atom that reduces the reactivity of the compound. Moreover, although a positive value of POCP_E indicates that ClBut contributes rising the tropospheric O₃ concentrations, the effect of this compound is very low as compare to the O₃ produced by the reference compound ethene.

The Ozone Depletion Potential (ODP) of a VOC is defined as the reduction in total ozone column per unit of mass emission for that compound relative to the reduction in total ozone column per unit of mass emission for trichlorofluoromethane (CFCl₃, often called CFC-11), and by definition the ODP for this compound is 1.0.⁴⁵ Thus, ODP provides an index of the relative ozone depletion to be expected from a compound of interest that can then be used in policy considerations. Because short-lived compounds, such as ClBut are not well-mixed throughout the troposphere, the ODPs depend not only on their atmospheric lifetime but also on the season and location of their emission. Therefore, model calculations are required to evaluate the ODPs of short-lived compounds. However, a simple procedure to estimate the ODPs seems to be also valuable. A semi-empirical approach has been

developed by Solomon and Albritton⁴⁶ and applied to the ODP estimation of a compound of interest from the following expression:

$$\text{ODP} = \frac{\tau_{\text{ClBut}}}{\tau_{\text{CFC13}}} * \frac{M_{\text{CFC13}}}{M_{\text{ClBut}}} * \frac{n_{\text{Cl}}}{3} \quad (\text{Eq. 11})$$

where M denotes the molecular weight of each species, n is the number of chlorine atoms in the considered VOC (the number 3 in the denominator represents the three chlorine atoms in CFC13 (CFC-11)), and τ_{ClBut} and τ_{CFC13} are the corresponding global atmospheric lifetimes. The value of τ_{CFC13} is taken as 45 years.⁴⁷ The obtained ODP value of 1.4×10^{-4} shows that this VOC must have a negligible effect on the stratospheric ozone depletion.

Finally, the contribution of the emission of ClBut to the greenhouse warming was estimated from the global warming potential (GWP), which indicates the possible climate impact of ClBut relative to the impact produced by the same amount of CO₂ over a given time horizon (TH) (usually 20 and 100 years) which is calculated according to Eq. 12.⁴⁸

$$\text{GWP}_{\text{ClBut}}(\text{TH}) = \frac{\text{AGWP}_{\text{ClBut}}(\text{TH})}{\text{AGWP}_{\text{CO}_2}(\text{TH})} \quad (\text{Eq. 12})$$

AGWP_{CO₂} is the absolute global warming potential of CO₂ (in W m⁻² year kg⁻¹), whose values are 2.46×10^{-14} and 9.17×10^{-14} W m⁻² year (kg CO₂)⁻¹ for THs of 20 and 100 years, respectively, as reported by Hodnebrog *et al.*⁴⁸ and AGWP_{ClBut} is the absolute global warming potential of ClBut (in W m⁻² year kg⁻¹) calculated according to the Eq. 13.

$$\text{AGWP}_{\text{ClBut}} = \text{RE}_{\text{ClBut}}^* \tau_{\text{ClBut}} * \left(1 - e^{-\frac{\text{TH}}{\tau_{\text{ClBut}}}} \right) \quad (\text{Eq. 13})$$

where RE_{ClBut} (in W m⁻² kg⁻¹) is the radiative efficiency due to a unit increase in the atmospheric abundance of ClBut and τ_{ClBut} is the atmospheric lifetime of this compound (in years).

The RE_{ClBut} (1.04×10^{-12} W m⁻² kg⁻¹) was determined according to the Pinnock method⁴⁹ from the IR absorption spectra recorded at 298 K in the spectral range (500-1500) cm⁻¹. Figure 5 shows the dependence of the absorption cross-section (in cm² molecule⁻¹) on the photon energy (in cm⁻¹) obtained averaging four IR spectra between 0.5 to 5.0 Torr of ClBut. The integrated absorption cross-section (1.83×10^{-17} cm² molecule⁻¹ cm⁻¹) was determined by integrating over the whole spectral range at intervals of 10 cm⁻¹.

The Pinnock method⁴⁹ is a good approximation to calculate the RE of compounds uniformly distributed in the atmosphere, which is not the case of compounds with short atmospheric lifetimes as in the case of ClBut. Hodnebbrog *et al.*⁴⁸ provided a correction factor $f(\tau)$ (Eq. 14) to the RE based on the atmospheric lifetime of the compound:

$$f(\tau) = \frac{a\tau^b}{1+c\tau^d} \quad (\text{Eq. 14})$$

where a , b , c and d are constants with values of 2.962, 0.9312, 2.994 and 0.9302, respectively. Then, considering $\tau_{\text{ClBut}} = 1.24 \times 10^{-2}$ years, the lifetime corrected radiative efficiency RE^* is $5.25 \times 10^{-14} \text{ W m}^{-2} \text{ kg}^{-1}$. Using $\text{RE}^* = \text{RE} \cdot f(\tau)$ in Eq. 13 and replacing the calculated value of $\text{AGWP}_{\text{ClBut}}$ in Eq. 12 the estimated values of $\text{GWP}(\text{TH})$ are 3.1×10^{-2} and 9.1×10^{-3} for THs of 20 and 100 years, respectively. Therefore, a negligible contribution to global warming is expected from ClBut as compare to the same amount of CO_2 .

All the estimated atmospheric indexes for ClBut are reported in Table 4.

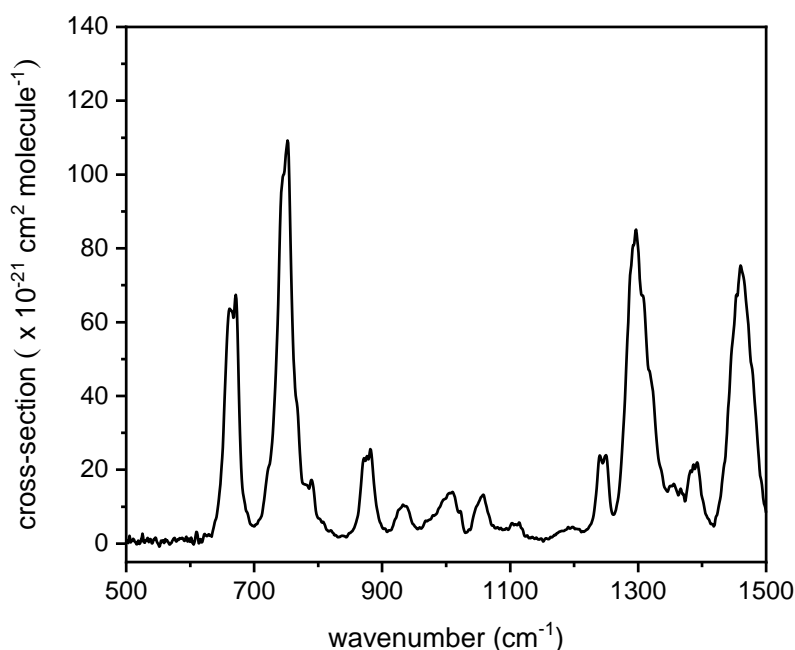


Figure 5. IR spectrum of ClBut at 298 K.

Table 4. Estimated atmospheric indexes of ClBut: global and coastal atmospheric lifetimes (τ_{global} and $\tau_{coastal}$), ozone depletion potential (ODP), modified photochemical ozone creation potentials index ($POCP_E$) for single and multi-days scales, radiative efficiency (RE) and lifetime corrected radiative efficiency (RE^*) and global warming potential (GWP) for time horizons of 20 and 100 years.

τ (years)		ODP	$POCP_E$		RE	RE^*	GWP	
<i>global</i>	<i>coastal</i>		<i>single day</i>	<i>multi days</i>	($W\ m^{-2}\ kg^{-1}$) / 10^{-12}		TH = 20 years	TH = 100 years
0.0124	0.0017	1.4×10^{-4}	10.55	20.68	1.04	0.0525	3.1×10^{-2}	9.1×10^{-3}

5. Conclusions

The rate coefficient for the reaction of ClBut with OH radicals was re-determined to be $(2.22 \pm 0.50) \times 10^{-12}\ cm^3\ molecule^{-1}\ s^{-1}$ at 296 K, using a relative method. The initial hydrogen abstraction process for this reaction was theoretically investigated at the (CCSD(T)/6-311++G(d,p)//BHandHLYP/6-311++G(d,p) level of theory and the reaction rate coefficient was calculated with the canonical transition state theory considering the reactivity and population of the different conformers of ClBut at 296 K, rendering a value $k_{theo} = 1.8 \times 10^{-12}\ cm^3\ molecule^{-1}\ s^{-1}$ in good agreement with the experimental one.

The reaction products were characterized for the first time which allows suggesting a likely reaction mechanism in clean atmospheres (absence of NOx). The main reaction products 4-chloro-2-butanone, 1-chloro-2-butanone and 1-chloro-2-butanol are obtained from the subsequent reaction of the alkyl radicals produced from the primary H-abstraction to C_γ and C_β of ClBut by the OH radical. The finding of 3-chloro-2-butanol could be associated to the isomerization of the missing primary product 4-chloro-2-butanol. On the other hand, the minor reaction products 3-hydroxy-butanaldehyde accounts for the reactivity of C_α , which is not negligible according to calculations.

The global atmospheric lifetime of ClBut was estimated at 4.9 days, indicating that this compound is rapidly degraded in the troposphere after being released and it may have only a local impact. Based on its $POCP_E$ values, we can infer that ClBut might contribute about 10 % to the production of tropospheric ozone compared to the contribution of the reference compound (ethene), under north-west Europe and the USA-urban conditions. Finally, as a result of its short global lifetimes and corrected lifetime radiative efficiencies, ClBut has small ODP and GWP values, so its emission into the atmosphere will not contribute significantly to either stratospheric ozone depletion or global warming of the Earth.

Supporting Information

TIC chromatogram for OH + ClBut reaction and mass spectrums of ClBut and corresponding products. Geometries of all stationary points in the reactive process and all relative energies including ZPE and thermal free energy corrections calculated at the BHandHLYP/6-311++G(d,p) level and refined at the CCSD(T)/6-311++G(d,p) level. Parameters used to calculate the POCP_E values.

Acknowledgments:

The authors wish to acknowledge CONICET, ANPCyT-FONCyT, SeCyT-UNC and MinCyT-Córdoba for the financial support of this work and to Sistema Nacional de Espectrometría de Masas. Dr. Juan Nájera (Laboratorio de Espectrometría de Masas of INFIQC) and Lic. Juana Salas are acknowledged for technical support and for recording IR spectra.

6. References

- (1) Kirschner, E. M. Environment, Health Concerns Force Shift In Use Of Organic Solvents. *Chem. Eng. News* **1994**, *72* (25), 13. <https://doi.org/10.1021/cen-v072n025.p013>.
- (2) Kirschner, E. M. Production of Top 50 Chemicals Increased Substantially in 1994. *Chem. Eng. News* **1995**, *73* (15), 16–20. <https://doi.org/10.1021/cen-v073n015.p016>.
- (3) Leisinger, T.; Brunner, W. Poorly Degradable Substances. In *Biotechnology*; Rehm, H. J., Reed, G., Eds.; Weinheim, 1986; pp 475–513.
- (4) Adriaens, P.; Gruden, C.; McCormick, M. L. Biogeochemistry of Halogenated Hydrocarbons. In *Treatise on Geochemistry*; Elsevier, 2014; Vol. 11, pp 511–533. <https://doi.org/10.1016/B978-0-08-095975-7.00914-1>.
- (5) SIDS Initial Assessment Report; OECD (Organization for Economic Co-Operation and Development). *SIDS Initial Assessment Report*, Paris, France, 1997.
- (6) Markert, F.; Nielsen, O. J. The Reactions of OH Radicals with Chloroalkanes in the Temperature Range 295-360 K. *Chem. Phys. Lett.* **1992**, *194* (1–2), 123–127. [https://doi.org/10.1016/0009-2614\(92\)85753-W](https://doi.org/10.1016/0009-2614(92)85753-W).
- (7) Loison, J. C.; Ley, L.; Lesclaux, R. Kinetic Study of OH Radical Reactions with Chlorobutane Isomers at 298K. *Chem. Phys. Lett.* **1998**, *296* (3–4), 350–356.

- 1
2
3 [https://doi.org/10.1016/S0009-2614\(98\)01058-6](https://doi.org/10.1016/S0009-2614(98)01058-6).
- 4
5 (8) Jara-Toro, R. A.; Hernández, F. J.; Taccone, R. A.; Lane, S. I.; Pino, G. A. Water
6 Catalysis of the Reaction between Methanol and OH at 294 K and the Atmospheric
7 Implications. *Angew. Chemie Int. Ed.* **2017**, *56* (8), 2166–2170.
8 <https://doi.org/10.1002/anie.201612151>.
- 9
10
11 (9) Jara-Toro, R. A.; Hernández, F. J.; Garavagno, M. de los A.; Taccone, R. A.; Pino, G.
12 A. Water Catalysis of the Reaction between Hydroxyl Radicals and Linear Saturated
13 Alcohols (Ethanol and n -Propanol) at 294 K. *Phys. Chem. Chem. Phys.* **2018**, *20*
14 (44), 27885–27896. <https://doi.org/10.1039/C8CP05411H>.
- 15
16
17 (10) Lendar, M.; Aissat, A.; Cazaunau, M.; Daële, V.; Mellouki, A. Absolute and Relative
18 Rate Constants for the Reactions of OH and Cl with Pentanols. *Chem. Phys. Lett.*
19 **2013**, *582*, 38–43. <https://doi.org/10.1016/j.cplett.2013.07.042>.
- 20
21
22 (11) Aranguren-Abrate, J. P.; Pisso, I.; Peirone, S. A.; Cometto, P. M.; Lane, S. I. Relative
23 Rate Coefficients of OH Radical Reactions with CF₃CFCClCF₃ and CF₃CHCH₂OH.
24 Ozone Depletion Potential Estimate for CF₃CFCClCF₃. *Atmos. Environ.* **2013**, *67*, 85–
25 92. <https://doi.org/10.1016/j.atmosenv.2012.10.047>.
- 26
27
28 (12) Barrera, J. A.; Garavagno, M. D. L. A.; Dalmaso, P. R.; Taccone, R. A. Atmospheric
29 Chemistry of 3-Methoxy-1-Propanol and 3-Methoxy-1-Butanol: Kinetics with OH
30 Radicals and Cl Atoms, Identification of the End-Products in the Presence of NO,
31 Mechanisms and Atmospheric Implications. *Atmos. Environ.* **2019**, *202* (January), 28–
32 40. <https://doi.org/10.1016/j.atmosenv.2018.12.056>.
- 33
34
35 (13) Calvert, J. G.; Derwent, R. G.; Orlando, J. J.; Tyndall, G. S.; Wallington, T. J.
36 *Mechanisms of Atmospheric Oxidation of the Alkanes*; Oxford University Press: New
37 York, 2008.
- 38
39
40 (14) IUPAC subcommittee for gas kinetic data evaluation. HO_x + CH₃CH(OH)CH₃
41 [http://iupac.pole-](http://iupac.pole-ether.fr/htdocs/datasheets/pdf/HOx_VOC26_HO_CH3CH(OH)CH3.pdf)
42 [ether.fr/htdocs/datasheets/pdf/HOx_VOC26_HO_CH3CH\(OH\)CH3.pdf](http://iupac.pole-ether.fr/htdocs/datasheets/pdf/HOx_VOC26_HO_CH3CH(OH)CH3.pdf). (accessed
43 Dec 6, 2019).
- 44
45
46 (15) Frisch, M. J.; Trucks, G. W.; Schlegel, H. B.; Scuseria, G. E.; Robb, M. A.;
47 Cheeseman, J. R.; Scalmani, G.; Barone, V.; Mennucci, B.; Petersson, G. A.; et al.
48 *Gaussian 09*, Revision D.01, Gaussian Inc.: Wallingford, CT. 2009.
- 49
50
51 (16) Alvarez-Idaboy, J. R.; Galano, A.; Bravo-Pérez, G.; Ruiz, M. E. Rate Constant
52 Dependence on the Size of Aldehydes in the NO₃ + Aldehydes Reaction. An
53 Explanation via Quantum Chemical Calculations and CTST. *J. Am. Chem. Soc.* **2001**,
54 *123* (34), 8387–8395. <https://doi.org/10.1021/ja010693z>.
- 55
56
57 (17) Galano, A.; Alvarez-Idaboy, J. R.; Ruiz-Santoyo, M. E.; Vivier-Bunge, A.
58 Glycolaldehyde + OH Gas Phase Reaction: A Quantum Chemistry + CVT/SCT
59
60

- 1
2
3 Approach. *J. Phys. Chem. A* **2005**, *109* (1), 169–180.
4 <https://doi.org/10.1021/jp047490s>.
5
6 (18) Eyring, H. The Activated Complex in Chemical Reactions. *J. Chem. Phys.* **1935**, *3* (2),
7 107–115. <https://doi.org/10.1063/1.1749604>.
8
9 (19) Evans, M. G.; Polanyi, M. Some Applications of the Transition State Method to the
10 Calculation of Reaction Velocities, Especially in Solution. *Trans. Faraday Soc.* **1935**,
11 *31* (708), 875–894. <https://doi.org/10.1039/TF9353100875>.
12
13 (20) Wigner, E. The Transition State Method. *Trans. Faraday Soc.* **1938**, *34*, 29–41.
14 <https://doi.org/10.1039/TF9383400029>.
15
16 (21) NIST mass spectral search program; ver. 2.0d.
17
18 (22) Ogawa, Y.; Imazeki, S.; Yamaguchi, H.; Matsuura, H.; Harada, I.; Shimanouchi, T.
19 Vibration Spectra and Rotational Isomerism of Chain Molecules. VII. 1-Chloro-, 1-
20 Bromo-, and 1-Iodopropanes, and 1-Chloro-, 1-Bromo-, and 1-Iodobutanes. *Bull.*
21 *Chem. Soc. Jpn.* **1978**, *51* (3), 748–767. <https://doi.org/10.1246/bcsj.51.748>.
22
23 (23) Melandri, S.; Caminati, W.; Favero, L. B.; Millemaggi, A.; Favero, P. G. A Microwave
24 Free Jet Absorption Spectrometer and Its First Applications. *J. Mol. Struct.* **1995**,
25 *352–353* (94), 253–258. [https://doi.org/10.1016/0022-2860\(94\)08516-K](https://doi.org/10.1016/0022-2860(94)08516-K).
26
27 (24) Fagerland, S.; Rydland, T.; Stølevik, R.; Seip, R. Conformation and Molecular
28 Structure of 1-Chlorobutane as Determined by Gas-Phase Electron Diffraction and
29 Molecular Mechanics Calculations. *J. Mol. Struct.* **1983**, *96* (3–4), 339–346.
30 [https://doi.org/10.1016/0022-2860\(83\)90061-3](https://doi.org/10.1016/0022-2860(83)90061-3).
31
32 (25) Aarset, K.; Hagen, K.; Stølevik, R.; Per Christian, S. Molecular Structure and
33 Conformational Composition of 1-Chlorobutane, 1-Bromobutane, and 1-Iodobutane as
34 Determined by Gas-Phase Electron Diffraction and Ab Initio Calculations. *Struct.*
35 *Chem.* **1995**, *6* (3), 197–205. <https://doi.org/10.1007/BF02286448>.
36
37 (26) Barnes, A. J.; Evans, M. L.; Hallam, H. E. Infrared Cryogenic Studies. Part 15.
38 Chloroalkanes in Argon Matrices. *J. Mol. Struct.* **1983**, *99* (3–4), 235–245.
39 [https://doi.org/10.1016/0022-2860\(83\)90026-1](https://doi.org/10.1016/0022-2860(83)90026-1).
40
41 (27) Kramer, Z. C.; Takahashi, K.; Skodje, R. T. Water Catalysis and Anticatalysis in
42 Photochemical Reactions: Observation of a Delayed Threshold Effect in the Reaction
43 Quantum Yield. *J. Am. Chem. Soc.* **2010**, *132* (43), 15154–15157.
44 <https://doi.org/10.1021/ja107335t>.
45
46 (28) Allodi, M. A.; Dunn, M. E.; Livada, J.; Kirschner, K. N.; Shields, G. C. Do Hydroxyl
47 Radical–Water Clusters, OH(H₂O)_n, n = 1–5, Exist in the Atmosphere? *J. Phys.*
48 *Chem. A* **2006**, *110* (49), 13283–13289. <https://doi.org/10.1021/jp064468l>.
49
50 (29) Finlayson-Pitts, B. J.; Pitts Jr, J. N. *Chemistry of the Upper and Lower Atmosphere:*
51 *Theory, Experiments, and Applications*; Oxford University Press USA: New York,
52
53
54
55
56
57
58
59
60

1999. <https://doi.org/10.1021/jp0363489>.
- (30) Jiménez, E.; Gierczak, T.; Stark, H.; Burkholder, J. B.; Ravishankara, A. R. Reaction of OH with HO₂NO₂ (Peroxynitric Acid): Rate Coefficients between 218 and 335 K and Product Yields at 298 K. *J. Phys. Chem. A* **2004**, *108* (7), 1139–1149. <https://doi.org/10.1021/jp0363489>.
- (31) Zhang, P.; Wang, W.; Zhang, T.; Chen, L.; Du, Y.; Li, C.; Lü, J. Theoretical Study on the Mechanism and Kinetics for the Self-Reaction of C₂H₅O₂ Radicals. *J. Phys. Chem. A* **2012**, *116* (18), 4610–4620. <https://doi.org/10.1021/jp301308u>.
- (32) Atkinson, R.; Baulch, D. L.; Cox, R. A.; Crowley, J. N.; Hampson, R. F.; Kerr, J. A.; Rossi, M. J.; Troe, J. *Summary of Evaluated Kinetic and Photochemical Data for Atmospheric Chemistry*; IUPAC Subcommittee on Gas Kinetic Data Evaluation for Atmospheric Chemistry, 2001.
- (33) Flick, E. W. *Industrial Solvents Handbook*; Industrial Solvents Handbook, Noyes Data Corporation: Westwood, New Jersey, U.S.A., 1998.
- (34) Atkinson, R.; Arey, J. Atmospheric Degradation of Volatile Organic Compounds. *Chem. Rev.* **2003**, *103* (12), 4605–4638. <https://doi.org/10.1021/cr0206420>.
- (35) Schubert, C. C.; Schubert, S. J.; Pease, R. N. The Oxidation of Lower Paraffin Hydrocarbons. I. Room Temperature Reaction of Methane, Propane, n-Butane and Isobutane with Ozonized Oxygen 1. *J. Am. Chem. Soc.* **1956**, *78* (10), 2044–2048. <https://doi.org/10.1021/ja01591a006>.
- (36) Wallington, T. J.; Skewes, L. M.; Siegl, W. O. A Relative Rate Study of the Reaction of Chlorine Atoms with a Series of Chloroalkanes at 295 K. *J. Phys. Chem.* **1989**, *93* (9), 3649–3651. <https://doi.org/10.1021/j100346a054>.
- (37) Prinn, R. G.; Huang, J.; Weiss, R. F.; Cunnold, D. M.; Fraser, P. J.; Simmonds, P. G.; McCulloch, A.; Harth, C.; Salameh, P.; O'Doherty, S.; et al. Evidence for Substantial Variations of Atmospheric Hydroxyl Radicals in the Past Two Decades. *Science*. **2001**, *292* (5523), 1882–1888. <https://doi.org/10.1126/science.1058673>.
- (38) Platt, U.; Janssen, C. Observation and Role of the Free Radicals NO₃, ClO, BrO and IO in the Troposphere. *Faraday Discuss.* **1995**, *100*, 175–198. <https://doi.org/10.1039/fd9950000175>.
- (39) Spicer, C. W.; Chapman, E. G.; Finlayson-Pitts, B. J.; Plastridge, R. A.; Hubbe, J. M.; Fast, J. D.; Berkowitz, C. M. Unexpectedly High Concentrations of Molecular Chlorine in Coastal Air. *Nature* **1998**, *394* (6691), 353–356. <https://doi.org/10.1038/28584>.
- (40) Jenkin, M. E.; Derwent, R. G.; Wallington, T. J. Photochemical Ozone Creation Potentials for Volatile Organic Compounds: Rationalization and Estimation. *Atmos. Environ.* **2017**, *163* (x), 128–137. <https://doi.org/10.1016/j.atmosenv.2017.05.024>.
- (41) Derwent, R. G.; Jenkin, M. E.; Saunders, S. M. Photochemical Ozone Creation

- 1
2
3 Potentials for a Large Number of Reactive Hydrocarbons under European Conditions.
4 *Atmos. Environ.* **1996**, *30* (2), 181–199. [https://doi.org/10.1016/1352-2310\(95\)00303-](https://doi.org/10.1016/1352-2310(95)00303-G)
5
6 G.
- 7
8 (42) Jenkin, M. E. *Photochemical Ozone and PAN Creation Potentials: Rationalisation and*
9
10 *Methods of Estimation*; Culham, Oxfordshire OX14 3DB, UK, 1998.
- 11 (43) Jenkin, M. E.; Derwent, R. G.; Wallington, T. J. Photochemical Ozone Creation
12
13 Potentials for Volatile Organic Compounds: Rationalization and Estimation. *Atmos.*
14
15 *Environ.* **2017**, *163* (x), 128–137. <https://doi.org/10.1016/j.atmosenv.2017.05.024>.
- 16 (44) Cheng, H. R.; Guo, H.; Saunders, S. M.; Lam, S. H. M.; Jiang, F.; Wang, X. M.;
17
18 Simpson, I. J.; Blake, D. R.; Louie, P. K. K.; Wang, T. J. Assessing Photochemical
19
20 Ozone Formation in the Pearl River Delta with a Photochemical Trajectory Model.
21
22 *Atmos. Environ.* **2010**, *44* (34), 4199–4208.
23
24 <https://doi.org/10.1016/j.atmosenv.2010.07.019>.
- 25 (45) Wuebbles, D. J. Chlorocarbon Emission Scenarios: Potential Impact on Stratospheric
26
27 Ozone. *J. Geophys. Res.* **1983**, *88* (C2), 1433.
28
29 <https://doi.org/10.1029/JC088iC02p01433>.
- 30 (46) Solomon, S.; Albritton, D. L. Time-Dependent Ozone Depletion Potentials for Short-
31
32 and Long-Term Forecasts. *Nature* **1992**, *357* (6373), 33–37.
33
34 <https://doi.org/10.1038/357033a0>.
- 35 (47) Forster, P.; Ramaswamy, V.; Artaxo, P.; Berntsen, T.; Betts, R.; Fahey, D. W.;
36
37 Haywood, J.; Lean, J.; Lowe, D. C.; Myhre, G.; et al. *Climate Change 2007: The*
38
39 *Physical Science Basis*; Climate Change 2007: The Physical Science Basis,
40
41 Cambridge University Press: Cambridge, U.K, 2007.
- 42 (48) Hodnebrog, Ø.; Etminan, M.; Fuglestvedt, J. S.; Marston, G.; Myhre, G.; Nielsen, C.
43
44 J.; Shine, K. P.; Wallington, T. J. Global Warming Potentials and Radiative
45
46 Efficiencies of Halocarbons and Related Compounds: A Comprehensive Review. *Rev.*
47
48 *Geophys.* **2013**, *51* (2), 300–378. <https://doi.org/10.1002/rog.20013>.
- 49 (49) Pinnock, S.; Hurley, M. D.; Shine, K. P.; Wallington, T. J.; Smyth, T. J. Radiative
50
51 Forcing of Climate by Hydrochlorofluorocarbons and Hydrofluorocarbons. *J. Geophys.*
52
53 *Res.* **1995**, *100* (D11), 23227–23238. <https://doi.org/10.1029/95JD02323>.
54
55
56
57
58
59
60

TOC graphic

